

An Arbitrary Waveform 16 Channel Neural Stimulator with Adaptive Supply Regulator in 0.35 μm HV CMOS for Visual Prosthesis

Jindeok Seo¹, Kyomuk Lim¹, Sangmin Lee², Jaehyun Ahn², Seokjune Hong², Hyungjung Yoo², Sukwon Jung^{2,3}, Sunkil Park², Dong-il “Dan” Cho², and Hyoungho Ko^{1,*}

Abstract—We describe a neural stimulator front-end with arbitrary stimulation waveform generator and adaptive supply regulator (ASR) for visual prosthesis. Each pixel circuit generates arbitrary current waveform with 5 bit programmable amplitude. The ASR provides the internal supply voltage regulated to the minimum required voltage for stimulation. The prototype is implemented in 0.35 μm CMOS with HV option and occupies 2.94 mm² including I/Os.

Index Terms—Neural stimulator, adaptive supply regulator (ASR), arbitrary waveform, visual prosthesis

I. INTRODUCTION

Over the past decades, visual prostheses based on functional electrical stimulation (FES) have been brought to great public attention for treating retinal degenerative diseases such as retinitis pigmentosa (RP) and age-related macular degeneration (AMD) [1]. The conceptual diagram of the visual prostheses is shown in Fig. 1. In the retinal structure of RP or AMD patients, the optic nerve is intact, however, the rods and cones are degenerated,

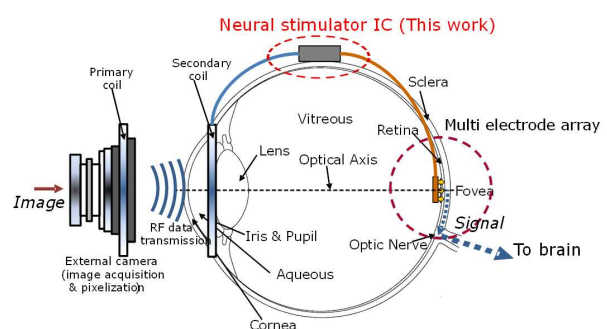


Fig. 1. Concept of visual prostheses.

thus the neural reaction is not occurred by the external light stimulation. The visual prostheses system using FES can bypass these defects, and can directly stimulate the optic nerve.

FES can be performed by either current or voltage stimulation pulses. Generally the current stimulation method is preferred over the voltage stimulation method in the visual prostheses because the current stimulation can accurately control the delivered amount of charge. The current stimulation, however, can generate quite high electrode voltages that may harm the tissues or damage the electrodes [2].

The current stimulators generally require high output voltage compliance, because the stimulators inject the biphasic current pulse with the maximum amplitude of several hundred μA into the microelectrodes and tissues of several tens $\text{k}\Omega$ impedance. For example, the output voltage compliance of 10 V ($= \pm 5$ V) is required to drive the 10 $\text{k}\Omega$ with the biphasic current pulse of ± 500 μA . Thus, the previous current stimulators are implemented

Manuscript received Jun. 5, 2012; revised Oct. 30, 2012.

¹Department of Electronics, Chungnam National University, Daejeon 305-764, Korea

²ASRI/ISRC, School of Electrical Engineering and Computer Science, Seoul National University, Seoul 151-744, Korea

³Medical IT Convergence Research Center, Korea Electronics Technology Institute, Seongnam 463-816, Korea

*E-mail of Corresponding Author : hhko@cnu.ac.kr

using high voltage (HV) CMOS process, and adopt the static high supply voltage of 5 to 35 V [1, 3-6]. Recently, neural stimulator with voltage compliance monitoring circuit for supply adaptation is reported [7], however, the circuit for controlling supply voltage is not included in [7].

The programmability of stimulation waveform is also one of the important issues. While most stimulators use biphasic current-mode rectangular waveforms, the neural researchers discover that the non-rectangular waveforms such as exponential, Gaussian and ramp, and so on, can provide more advanced neural stimulation effect [8]. The previous researches show that different types of applications need different stimulation waveforms in order to produce an optimum stimulation effect [7, 8]. For example, the repeated pulse train was more effective than single pulse stimulation. The asymmetric biphasic pulses have been proven to limit channel interaction between adjacent stimulation sites, and avoid new excitation during the discharge phase. The exponential decrease can reduce the tissue damage. The interphase delay can provide stronger stimulation effects. Recently the neural stimulator with arbitrary programmable pulse shape is reported [8].

This paper proposes a 16 channel arbitrary waveform current stimulator front-end with the adaptive supply

voltage regulator (ASR) for the visual prosthesis, as shown in Fig. 2. Each stimulator pixel circuit includes decoding logics, 5 bit digital to analog converter (DAC), biphasic electrode driver and ASR. Each pixel circuits can generate the arbitrary stimulation waveform using the received data packets from global data bus.

In the proposed circuit, the internal power supply voltage is not static, but adaptively regulated to the minimum required voltage for stimulation, thus current stimulation with lower voltage than previous static HV stimulators can be achieved. The ASR provides the adaptively regulated internal supply voltage using current feedback loop. Moreover, the current feedback loop, which monitors the stimulating current and feeds back the monitored current to the regulator, gives the robustness to the variations of the load impedances.

II. SYSTEM DESIGN

1. Top Level Operation

The system consists of the reference circuit, control logic and the 16 channel (4 by 4) stimulator pixel circuit arrays. The each pixel circuit includes digital logic, 5 bit digital to analog converter (DAC) and biphasic current driver with the ASR. The timing diagram of the system is

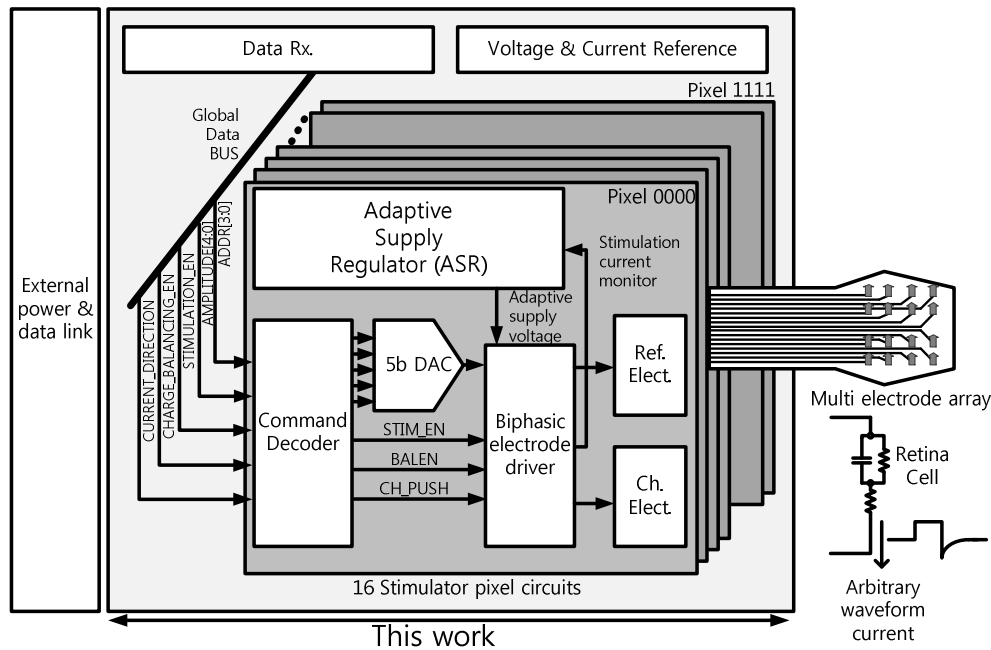


Fig. 2. Top-level block diagram of stimulator front-end.

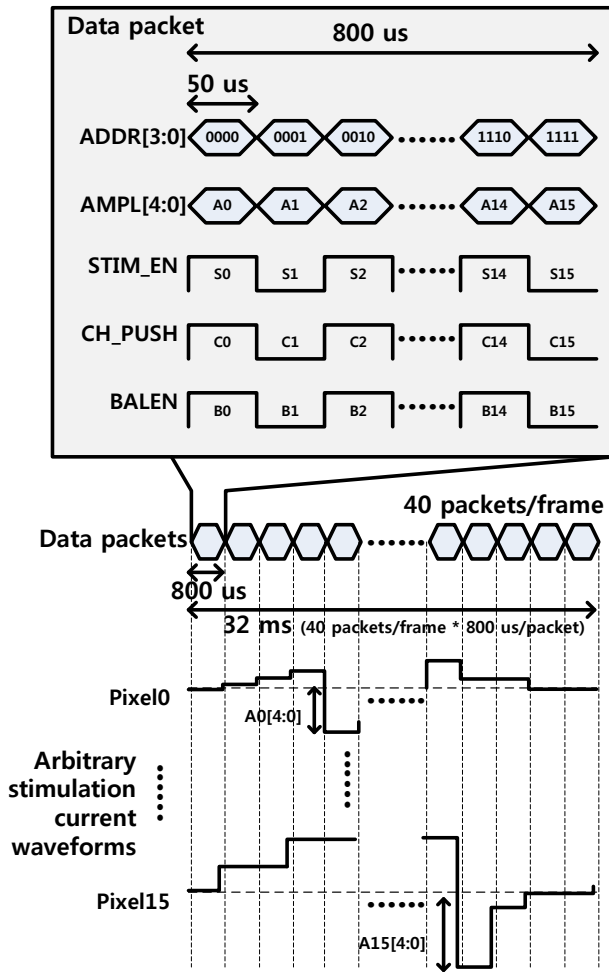


Fig. 3. Timing diagram.

given in Fig. 3. A data packet, which determines the current status of 16 channel stimulation pixels, includes the stimulation address, stimulation amplitude, stimulation enable, stimulation direction, and charge balancing enable signals. The default stimulation period of single data packet is 800 μs. The 4 bit address signal, ADDR[3:0], determines which pixel is stimulated. In the data packet, ADDR[3:0] is increased from “0000” to “1111”. The amplitude of the stimulation current is determined using 5 bit amplitude signal, AMPL[4:0]. The STIM_EN determines whether the stimulation of the target pixel is enabled or not. The CH_PUSH determines whether the direction of the stimulation current is push or sink. After the stimulation, the passive charge balancing operation is performed using BALEN. Each pixel circuit includes the decoder and flip-flops, and keeps the current status until the next commands are applied, and the arbitrary waveform per individual pixel can be generated.

2. Current Stimulator with Adaptive Supply Regulator

The schematic of the proposed biphasic current stimulator with ASR is shown in Fig. 4. The operation status of the stimulator is determined by the input signals, STIM_EN, CH_PUSH and BALEN. When STIM_EN is ‘H’, this circuit is activated. The direction of the stimulating current is determined by CH_PUSH. When CH_PUSH is ‘H’, the current flows in forward direction, from channel electrode to reference electrode. When CH_PUSH is ‘L’, the current flows in backward direction, from reference electrode to channel electrode. After the stimulation, the charge balancing, which is to prevent the electrolytic damage by the remaining charge, is enabled by BALEN.

When CH_PUSH = ‘H’, for example, the stimulation current flows through PM2 - channel electrode - retina cell - reference electrode - NM7. If the required output voltage compliance is high, due to the high stimulation current or the large impedance between electrodes, the sourcing current source (PM2) cannot be operated in saturation region, while sourcing current monitor (PM3) is in saturation region. The actual stimulation current of NM7 is monitored by sinking current monitor (NM8), which is in saturation region. In anodic stimulation, I_{DS} of PM3 and I_{DS} of NM8 mean the desired current and monitored current, respectively. The current difference, which is the subtraction of the monitored current from desired current, is fed back to the supply regulator. This feedback loop increases the internal supply voltage when the monitored current is smaller than the desired current, and reduces the internal supply voltage when the

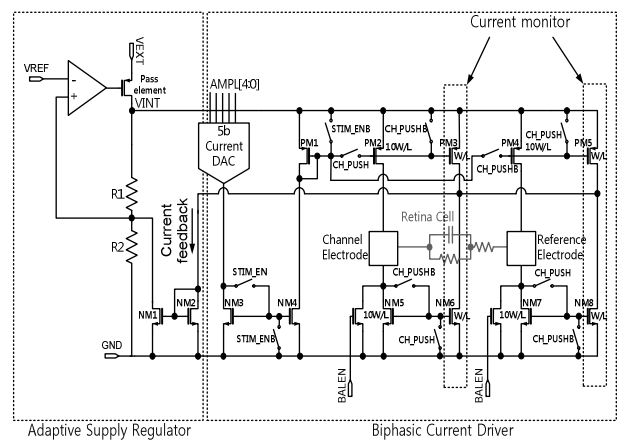


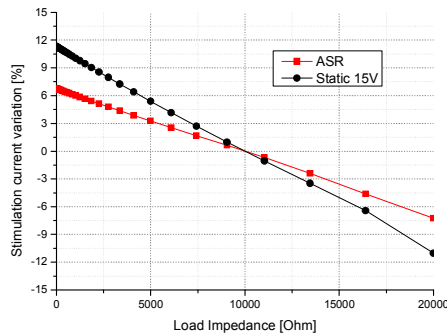
Fig. 4. Stimulator pixel circuit.

monitored current is higher than the desired current. Thus, the internal supply is adaptively regulated to the minimum required supply voltage using this current feedback loop. Also, the current feedback loop gives the robustness to the variations of the load impedances.

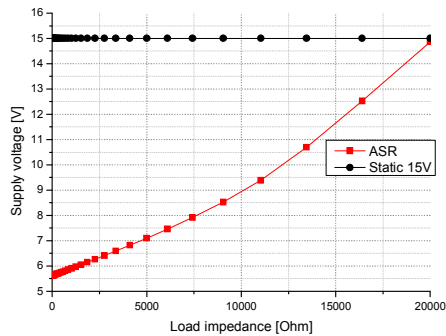
The simulation results of stimulation current variation and adaptive supply voltage with varying load impedance are shown in Fig. 5(a) and Fig. 5(b), respectively. In this simulation, the stimulation current amplitude, AMPL[4:0] is set to “10000”, and the load impedance is increased from 0 Ohm to 20 kOhm. In Fig. 5(a), the stimulation current variation of the ASR stimulator is from +6.75 % to -7.25 %, while the stimulation current variation of the conventional stimulator with static 15 V supply is from +11.30 % to -11.03 % with the load impedance variation from 0 Ohm to 20 kOhm. Fig. 5(b) shows the simulated internal supply voltage of ASR. The internal supply voltage of ASR is increased from 5.6 V to 15 V.

III. PROTOTYPE MEASUREMENTS

The die photograph of the fabricated stimulator chip is shown in Fig. 6(a). The chip is fabricated in $0.35\ \mu\text{m}$

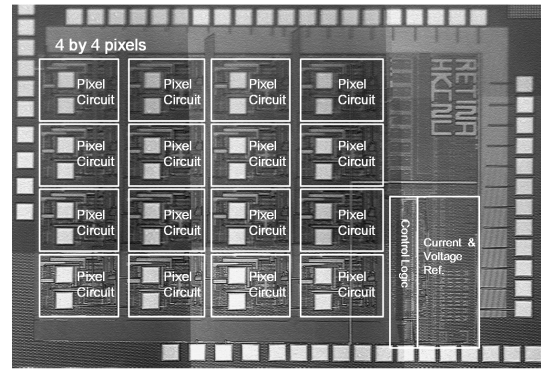


(a) Stimulation current variation vs. load impedance

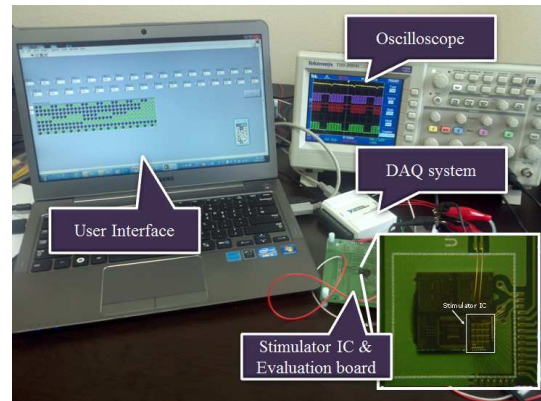


(b) Adaptive supply voltage vs. load impedance

Fig. 5. Simulation results.



(a) Die photograph



(b) Measurement setup

Fig. 6. Fabrication results.

CMOS with HV option and occupies $2.94\ \text{mm}^2$ including I/O pads. The single pixel circuit consumes $0.12\ \text{mm}^2$. With this pixel circuit, 256 channel stimulator can be realized on less than $6 \times 6\ \text{mm}^2$, which is feasible for implantation. The measurement setup is shown in Fig. 6(b). The fabricated chip is directly wire-bonded to the evaluation board (chip-on-board). The stimulation data packets are generated using user interface and data acquisition (DAQ) system.

With the external HV supply of 15 V and load impedance of $10\ \text{k}\Omega$, the measured internal supply voltage of ASR and stimulation current is shown in Fig. 7. When the input code of AMPL[4:0] is increased from “00000” to “11111”, the stimulation current is increased from $0\ \mu\text{A}$ to $880\ \mu\text{A}$, and the adaptive supply voltage is increased from 5.6 V to 15 V.

Fig. 8 shows the measured and simulated stimulation current with varying load impedance. Here, the stimulation current amplitude, AMPL[4:0] is set to “10000”. The measured stimulation current is smaller than simulated current of $22\ \mu\text{A}$ at $10\ \text{k}\Omega$ load

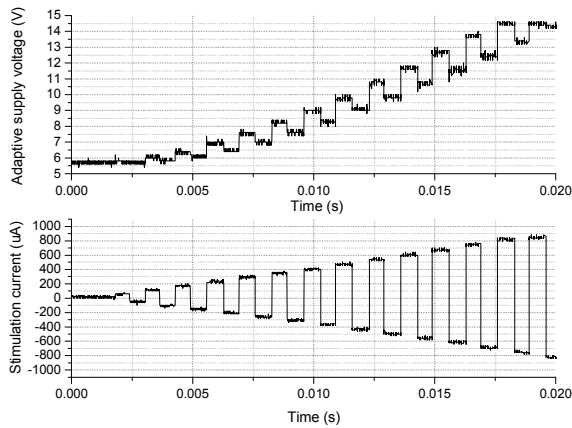


Fig. 7. Measured adaptive supply voltage and stimulation current.

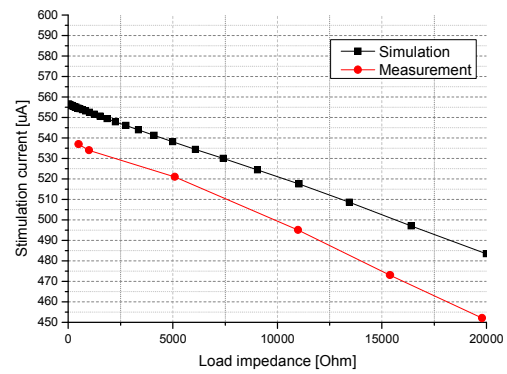
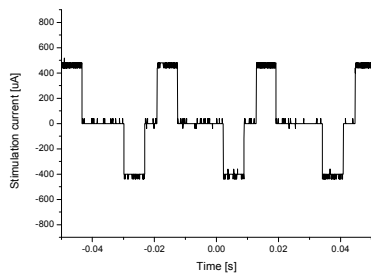
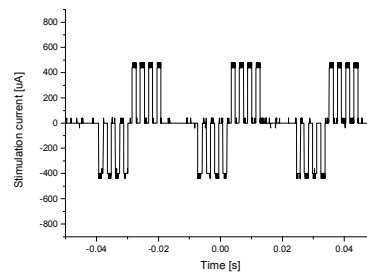


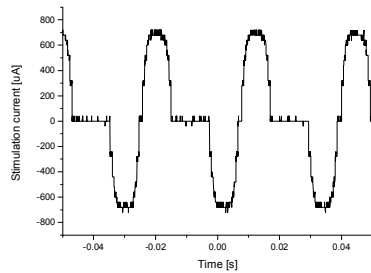
Fig. 8. Stimulation current with varying load impedance.



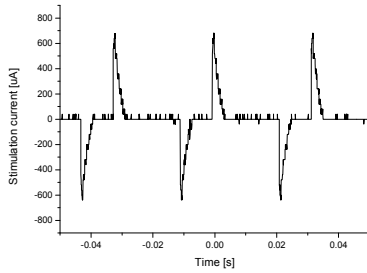
(a) Biphasic square waveform with interphase delay



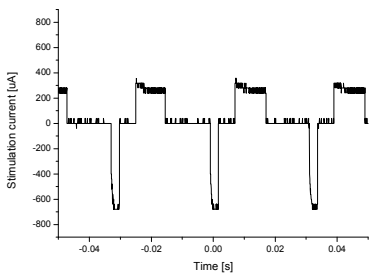
(b) Biphasic repeated pulse train waveform



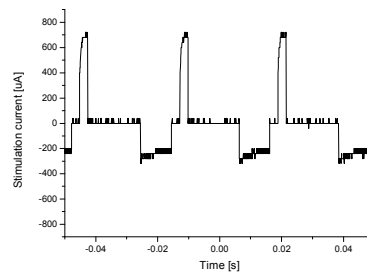
(c) Sinusoidal waveform



(d) Exponential cathodic and anodic waveform



(e) Fast cathodic pulse and slow anodic pulse



(f) Fast anodic pulse and slow cathodic pulse

Fig. 9. Various stimulation waveforms generated by fabricated circuit.

impedance. The measured variation of stimulation current is from +8.04 % to -9.05 %, while the simulated variation is from +6.75 % to -7.25 %, with the load impedance variation of 0 Ohm to 20 kOhm.

Fig. 9 shows the various stimulation current waveforms generated by the fabricated stimulator, which include biphasic square waveforms with interphase delay (Fig. 9(a)), biphasic repeated pulse train waveform (Fig.

Table 1. Comparison with previous stimulators

	[1]	[5]	[6]	[7]	This work
# of pixels	256	15	232	2	16
Static power consumption (Full chip)	1.45 mW	3.2 mW	8 mW	1.16 mW	7.68 mW
Dynamic power consumption	Pattern dependent	Pattern dependent	Pattern dependent	Pattern dependent	Pattern dependent (max 328.3 mW)
Stimulation voltage	± 12 V	± 2.5 V	22.5 V (typ) 35 V (max)	20 V	Max 15 V (adaptive)
Stimulation voltage adaptation	Static supply	Static supply	Static supply	Compliance monitor for supply adaption	Adaptive supply regulation
Process	0.18 μ m HV	0.5 μ m HV	0.35 μ m HV	0.35 μ m HV	0.35 μ m HV
Full scale stimulation current	500 μ A	960 μ A	992 μ A	1000 μ A	880 μ A
Current DAC Resolution	4 bit	5 bit	5 bit	5 bit	5 bit
Wave-shape programmability	Biphasic rectangular waveform	Biphasic rectangular waveform	Biphasic rectangular waveform	Arbitrary waveform	Arbitrary waveform
Pixel size (mm ²)	0.08	N/A	0.1	0.2	0.12
Chip size (mm ²)	27.03	5.29	22	N/A	2.94

9(b)), sinusoidal waveform (Fig. 9(c)), exponential cathodic and anodic waveform (Fig. 9(d)), imbalanced fast cathodic pulse and slow anodic pulse (Fig. 9(e)), imbalanced fast anodic pulse and slow cathodic pulse.

The comparison with previous stimulators is given in Table 1. Compared to the previous stimulators, the supply adaptation and wave-shape programmability are main advantage of this work. However, the high static power consumption of 7.68 mW, which is mainly due to the standby current of ASR, is drawback. In the next version of stimulator, the static power consumption will be reduced by adding low power standby mode to ASR.

IV. CONCLUSIONS

A 16 channel, 5 bit controllable arbitrary waveform neural stimulator front-end IC with ASR is developed. Each pixel circuit can generate the stimulation current with programmable wave-shape. The more advanced neural stimulation effect for visual prosthesis can be achieved with this high wave-shape programmability. The internal supply of the each stimulator pixel is adaptively regulated by ASR. The ASR enables the lower voltage stimulation than conventional static HV supply stimulator when the required voltage compliance is small. Also, the ASR gives the robustness to the variations of the load impedances.

ACKNOWLEDGMENTS

This research was supported by the Happy tech. program through the National Research Foundation of Korea (NRF) funded by the Ministry of Education, Science and Technology (2012-0008611). This work was also supported by IC Design Education Center (IDEC).

REFERENCES

- [1] K. Chen, Z. Yang, L. Hoang, J. Weiland, M. Humayun, and W. Liu, "An Integrated 256-Channel Epiretinal Prosthesis," *Solid-State Circuits, IEEE Journal of*, Vol. 45, No. 9, pp. 1946-1956, Sep., 2010.
- [2] P. Livi, F. Heer, U. Frey, D. J. Bakkum, and A. Hierlemann, "Compact Voltage and Current Stimulation Buffer for High-Density Microelectrode Arrays," *IEEE Transactions on Biomedical Circuits and Systems*, Vol. 4, No. 6, pp. 372-378, Dec., 2010.
- [3] I. Kim, J. Song, Y. Zhang, T. Lee, T. Cho, Y. Song, D. Kim, S. Kim, and S. Hwang, "Biphasic electric current stimulates proliferation and induces VEGF production in osteoblasts," *Biochimica et Biophysica Acta (BBA) - Molecular Cell Research*, Vol. 1763, No. 9, pp. 907-916, Sep., 2006.
- [4] T. Tokuda, K. Hiyama, S. Sawamura, K. Sasagawa, Y. Terasawa, K. Nishida, Y. Kitaguchi, T. Fujikado,

Y. Tano, J. Ohta, "CMOS-Based Multichip Networked Flexible Retinal Stimulator Designed for Image-Based Retinal Prosthesis," *Electron Devices, IEEE Transactions on*, Vol. 56, No. 11, pp. 2577-2585, Nov., 2009.

- [5] L. Theogarajan, "A Low-Power Fully Implantable 15-Channel Retinal Stimulator Chip," *Solid-State Circuits, IEEE Journal of*, Vol. 43, No. 10, pp. 2322-2337, Nov., 2008.
- [6] M. Ortmanns, A. Rocke, M. Gehrke, H. Tiedtke, "A 232-Channel Epiretinal Stimulator ASIC," *Solid-State Circuits, IEEE Journal of*, Vol. 42, No. 12, pp. 2946-2959, Dec., 2007.
- [7] E. Noorsal, K. Sooksood, H. Xu, R. Hornig, J. Becker, M. Ortmanns, "A Neural Stimulator Frontend With High-Voltage Compliance and Programmable Pulse Shape for Epiretinal Implants," *Solid-State Circuits, IEEE Journal of*, Vol. 47, No. 1, pp. 244-256, Jan., 2012.
- [8] D. R. Merrill, M. Bikson, and J. G. Jefferys, "Electrical stimulation of excitable tissue: Design of efficacious and safe protocols," *Journal of Neuroscience Methods*, Vol. 141, pp. 171-198, Feb., 2005.



Jindeok Seo received the B.S. degree in the Department of Electronics from Chungnam National University, Daejeon, Korea, in 2011. Currently, he is pursuing the M.S. degree in the Department of Electronics from Chungnam National

University, Daejeon, Korea. His research interests include CMOS biomedical circuit design and analog-to-digital converters.



Kyomuk Lim received the B.S. degree in the Department of Electronics from Chungnam National University, Daejeon, Korea, in 2011. Currently, he is pursuing the M.S. degree in the Department of Electronics from Chungnam National

University, Daejeon, Korea. His research interests include CMOS biomedical circuit design and analog-to-digital converters.



Sangmin Lee received the BS degree in the School of Electrical Engineering and Computer Sciences, Seoul National University, Seoul, Korea, in 2005. Currently he is a PhD candidate student in the School of Electrical Engineering and Computer Sciences, Seoul National University, Seoul, Korea.



Jae Hyun Ahn received his B.S. and M.S. degrees in Electrical Engineering from Oklahoma State University, USA in 2000 and 2002 respectively. He was also with Samsung System LSI from 2002 to

2008, where he was involved in the analog front-end design for optical disk products. He is currently working towards his Ph.D. in the School of Electrical Engineering and Computer Science at Seoul National University, Korea.



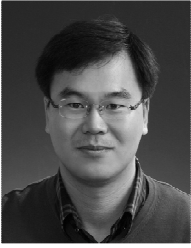
Seok-jun Hong received the B.S. and M.S. degree in the School of Electrical Engineering from Seoul National University, Korea, in 2009 and 2011 respectively. He is currently pursuing the Ph.D. degree in the Department of Electrical

Engineering from Seoul National University, Korea. His interests include MEMS fabrication and applications.



Hyung Jung Yoo received the BS degree in the School of Electrical Engineering and Computer Science, Kyungpook National University, Daegu, Korea, in 2010 and M.S. degree in the School of Electrical Engineering and Computer Science,

Seoul National University, Seoul, Korea, in 2012. Currently he is Ph.D. candidate in the School of Electrical Engineering and Computer Science, Seoul National University, Seoul, Korea.



Suk Won Jung received the B.S. degree and M.S. degree in the Department of Electronics Engineering from the University of Seoul, Korea, in 1994 and 1996, respectively. He is currently pursuing the Ph.D. degree in the Department

of Electrical and Computer Science Engineering from Seoul National University, Korea. And he is working for Korea Electronics Technology Institute (KETI) as a managerial researcher. His interests include artificial retinal prosthetic devices, highly sensitivity photonic devices and their application to medical instruments.



Dong-il "Dan" Cho received his BSME degree from Carnegie–Mellon University, Pittsburgh, PA, in 1980 and the M.S. and Ph. D. degrees from Massachusetts Institute of Technology, Cambridge, in 1984 and 1987, respectively. From 1987 to

1993, he was an Assistant Professor in the Mechanical and Aerospace Engineering Department, Princeton University, Princeton, NJ. In 1993, he joined the Department of Control and Instrumentation Engineering, Seoul National University, Seoul, South Korea, where he is currently Professor in the School of Electrical Engineering and Computer Science.



Sunkil Park received his BS degree in mechatronics engineering from Korea University of Technology and Education, Chunan, Korea, in 2003 and M.S. degrees in the School of Electrical Engineering and Computer Science at Seoul National University,

Korea, in 2007, respectively. He is currently pursuing the Ph.D. degree in the School of Electrical Engineering and Computer Science at Seoul National University, Korea. His research interest includes the design and fabrication of microactuator and prosthetic devices.



Hyoungho Ko received his BS and Ph. D. degrees in the School of Electrical Engineering from Seoul National University, Korea, in 2003 and 2008, respectively. He was with Samsung Electronics as a senior engineer from 2008 to 2010. In 2010,

he joined the Department of Electronics, Chungnam National University, Daejeon, Korea, where he is currently assistant professor. His interests include CMOS analog integrated circuit design.